Available online at www.sciencedirect.com
ScienceDirect
Journal of Colloid and Interface Science 304 (2006) 261–270
JOURNAL OF Colloid and Interface Science
www.elsevier.com/locate/jcis

Versatile transmission ellipsometry to study linear ferrofluid magneto-optics

E.S. Kooij *, A.C. Gâlcă, B. Poelsema

Solid State Physics group, MESA+ Institute for Nanotechnology, University of Twente, P.O. Box 217, 7500AE Enschede, The Netherlands

Received 24 July 2006; accepted 30 August 2006

Available online 8 September 2006

Abstract

Linear birefringence and dichroism of magnetite ferrofluids are studied simultaneously using spectroscopic ellipsometry in transmission mode. It is shown that this versatile technique enables highly accurate characterisation of magneto-optical phenomena. Magnetic field-dependent linear birefringence and dichroism as well as the spectral dependence are shown to be in line with previous results. Despite the qualitative agreement with established models for magneto-optical phenomena, these fail to provide an accurate, quantitative description of our experimental results using the bulk dielectric function of magnetite. We discuss the results in relation to these models, and indicate how the modified dielectric function of the magnetite nanoparticles can be obtained.

Keywords: Spectroscopic ellipsometry; Magneto-optics; Magnetite nanoparticles; Ferrofluids

1. Introduction

Many different application fields have benefited from the characteristic properties of ferrofluids. These liquids typically consist of metallic (Fe, Ni or Co) cubic spinel oxidic single-domain ferro- or ferrimagnetic nanoparticles, suspended in polar or non-polar solvents using suitable surfactants. Ferrofluids are used in mechanical devices, such as seals, bearings and dampers, and also in electromechanical devices such as loudspeakers, stepper motors and sensors. They have also been employed as a material for non-destructive testing of components such a magnetic tapes, stainless steels and turbine blades.

The optical properties of ferrofluids under the application of an external magnetic field are subject of substantial research efforts, ultimately aimed at incorporating the optically active ferrofluids in applications such as optical shutters, switches, and tuneable polarizing or phase-changing elements. The transition from an optically isotropic material to an (optically) anistropic medium was first observed by Majorana [1,2] in colloids as the magnetic equivalent of the electrical Kerr effect. Shortly after this, Cotton and Mouton [3] observed similar magnetically induced birefringence and dichroism in liquids. Consequently, these tuneable optical phenomena are often referred to as Cotton–Mouton effects.

Well-described synthesis procedures [4–8], and also the commercial availability of a wide variety of ferrofluids has stimulated scientific research in this field. Both experimental and theoretical work is focused on elucidating the origin of the magneto-optical properties of these suspensions and exploring their applicability as active optical devices [9–27]. Initially, the theoretical description of the magneto-optical properties of ferrofluids was based on the alignment of slightly non-spherical particles with uniaxial magnetic anisotropy in an applied magnetic field [9]. The magnetically induced optical anisotropy was attributed to the shape anisotropy of the prolate ellipsoidal particles with different polarizabilities along their short and long axes [9,16]. The possible contribution of pre-existing aggregates, or conglomerates formed in the applied field have been discussed and investigated [11–14,18]. Linear chains consisting of many particles have also been considered as a possible explanation for the magneto-optical properties [15]. Finally, Raşa presented a general theory for all magneto-optical phenomena due to non-interacting particles, in which the dielectric tensor of the ferrofluid is considered [21,22].

The magneto-optical properties of ferrofluids have been investigated in the past with a number of different experimen-

* Corresponding author.
E-mail address: e.s.kooij@utwente.nl (E.S. Kooij).
URL: ssp.tnw.utwente.nl (E.S. Kooij).

0021-9797/$ – see front matter
doi:10.1016/j.jcis.2006.08.062

tal set-ups [9,10,14,17–20,22]. Most often only birefringence is considered, and the magnetically induced dichroism is neglected. However, in some cases both aforementioned quantities are obtained, at a single wavelength or over a larger spectral range, but in the analysis the quantitative relation between the birefringence and the dichroism is not considered. In this work we study both linear magneto-optical quantities of an oil-based ferrofluid in the presence of a homogeneous magnetic field. We demonstrate the versatility of spectroscopic ellipsometry in transmission mode for simultaneously measuring the linear magneto-optical quantities with high accuracy. The relations between the ellipsometric quantities Ψ and Δ on one hand and the birefringence and dichroism on the other hand, are derived. In a final section, the results are discussed in relation to previous work and theoretical models, which describe magneto-optical behaviour.

2. Ferrofluid synthesis and characterisation

2.1. Synthesis

All measurements described in this paper are done using oleic acid stabilized magnetite (Fe_3O_4) suspensions, synthesized by reduction of ferrous and ferric chloride by ammonium hydroxide as for example described by van Ewijk et al. [6]. In a typical synthesis, 1.3 g $FeCl_3$ and 0.5 g $FeCl_2$ are dissolved in 80 ml of demineralised water. While stirring vigorously, 5 ml 25% NH_3 is added, resulting in a black precipitate. The magnetite is precipitated using a magnet and the supernatant is discarded, after which it is washed at least 4 times in demineralised water, until the solution pH is 7. Subsequently, 50 ml of demineralised water and 50 ml of oleic acid are added to the washed precipitate, and the mixture is stirred for at least 30 min while heating to 50 °C. After cooling of the mixture, the water is removed, and 50 ml of acetone is added. Using a magnet, the magnetite is precipitated and the supernatant is discarded. This washing procedure is repeated at least 4 times, after which the acetone is removed from the black substance by moderate heating. Finally, 50 ml cyclohexane is added to the dried residue to yield a suspension with a volume fraction of approximately $\Phi_0 = 1.56 \times 10^{-3}$.

2.2. Characterisation

A typical TEM image of the as-prepared magnetite ferrofluid, obtained using a Philips CM30 Twin/STEM system with a standard carbon-coated copper grid, is shown in Fig. 1.

As can be seen, the shape of the magnetite nanoparticles is very irregular. To assess the size dispersion and shape anisotropy, TEM images are analysed by determining the long and short axes of a large number of particles. The resulting histograms of both short and long axes are shown in Figs. 2a and 2b, respectively.

Assuming a normal distribution, the average diameter $\bar{d}$ for the short and long axes amount to 5.9 and 7.7 nm, respectively. The polydispersity $100\% \cdot \sigma/\bar{d}$ of both distributions is approximately 30%, with $\sigma = \sqrt{\overline{d^2} - \bar{d}^2}$ the standard deviation. In addition to what is clearly observed in Fig. 1, this indicates that the suspension is far from monodisperse. For a monodisperse suspension, the polydispersity parameter is generally required to be less than 5%, or at most 10% [28]. Often the particle size distributions are considered to follow a log-normal distribution [19,22], given by

$$f(d) = \frac{1}{s \cdot d \cdot \sqrt{2\pi}} \exp\left(-\frac{\ln^2(d/d_0)}{2s^2}\right), \tag{1}$$

where $\ln(d_0)$ and s are the mean value and standard deviation of $\ln(d)$. The solid lines in Fig. 2 show the log-normal functions obtained from the distributions. For the short and long diameters, $d_0 = 5.6$ and 7.4 nm are obtained, while the standard deviation amounts to $s = 0.31$ for both distributions. These

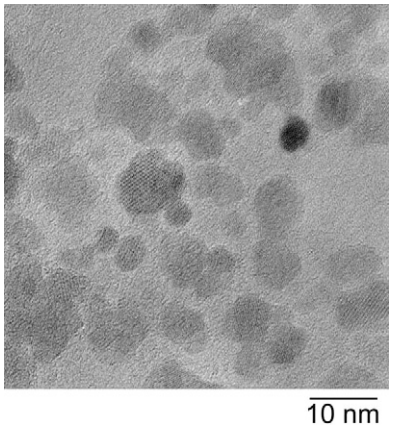

Fig. 1. TEM image of Fe_3O_4 nanoparticles in a magnetite ferrofluid, synthesized as described in the text.

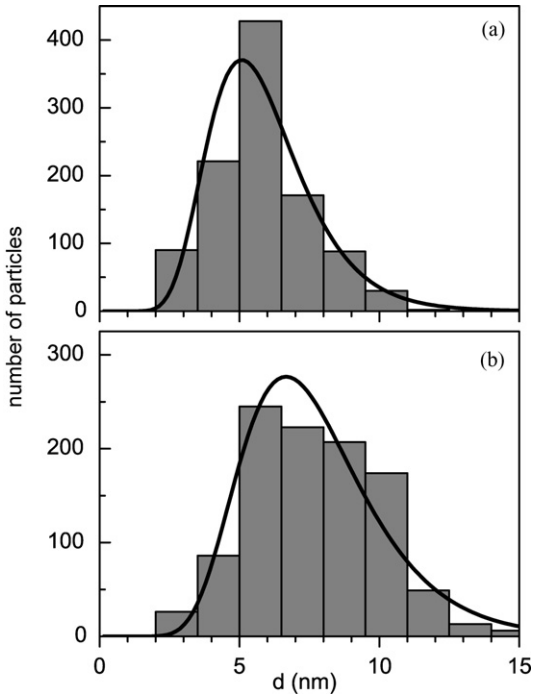

Fig. 2. Size distribution of the short (a) and long (b) diameters of the Fe_3O_4 nanoparticles as determined from TEM images such as the one in Fig. 1.

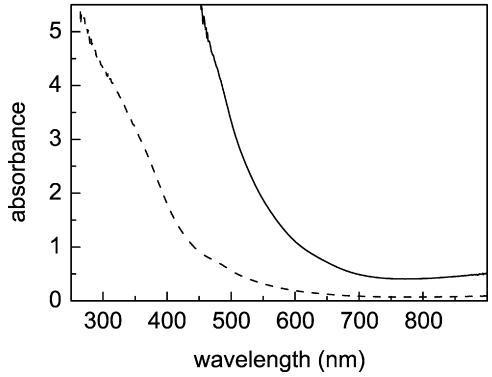

Fig. 3. UV–vis absorbance spectra of Fe_3O_4 ferrofluids as used in this work. As-prepared suspensions were diluted to yield fill fractions of $\Phi = 1.56 \times 10^{-4}$ and 2.60×10^{-5} ((—) and (- - -), respectively).

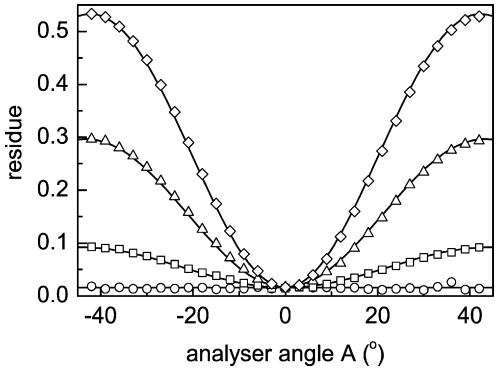

Fig. 4. Residue calibration curves for different values of the externally applied magnetic field. In the absence of a magnetic field the residue is independent of the analyser angle A, indicated by (○). (□), (△) and (◇) correspond to magnetic flux densities of 0.014, 0.025 and 0.039 T, respectively. (—) represent fit results obtained using Eq. (3). The calibration was performed at 600 nm, while the fill fraction was $\Phi = 3.60 \times 10^{-4}$.

parameters will be employed in the analysis of the magneto-optical properties.

To assess the optical properties of isolated particles, UV–vis absorbance[1] spectra were recorded on a Varian Cary 300 Scan spectrophotometer in double-beam mode, using a 1 cm cuvette filled with only the solvent (cyclohexane) as reference.

The ferrofluid appearance is dark brown to black, even for moderate fill fractions. This is also observed in the spectra in Fig. 3. For the relatively high fill fraction ($\Phi = 1.56 \times 10^{-4}$, solid line) the absorbance exceeds the experimentally available range for wavelengths below approximately 500 nm. Considerably more diluted suspensions still exhibit the strong increase of the absorbance towards shorter wavelengths.

3. Linear magneto-optics

3.1. Transmission ellipsometry setup

Magneto-optical properties are investigated using a home-built rotating polariser spectroscopic ellipsometer, equipped with a Xe lamp, a rotating polariser, fixed analyser and a scanning monochromator [29]. Measurements are performed in the visible region of the spectrum. Standard quartz spectrometer cuvettes (Starna) with optical path lengths of 1.0 and 10 mm are used. A cuvette is placed in a homogeneous DC magnetic field generated between the poles of a home-built water-cooled electromagnet, connected to a Delta Elektronika SM3540 power supply. The direction of the applied magnetic field is in all cases perpendicular to the light propagation direction, allowing only the determination of linear magneto-optical birefringence and dichroism.

The incident light is linearly polarised, which upon transmission through an anisotropic medium is generally transformed to elliptically polarised light. The complex transmission coefficient ρ is defined through

$$\rho = \frac{t_p}{t_s} = \tan(\Psi)\exp(i\Delta), \tag{2}$$

where t_p and t_s are the transmission coefficients for parallel and perpendicular polarisations, respectively [30]. In reflection ellipsometry, the polarisation directions are defined with respect to the plane of reflection, spanned by the incoming and outgoing light beams. Prior to a measurement, the azimuthal angles of the optical components, such as the polariser, the analyser and possibly a compensator, are accurately calibrated with respect to this plane of reflection. In the absence of a magnetic field, the ferrofluid in the cuvette is isotropic and, since we are using the ellipsometer in transmission mode, such a reference plane can not be defined. However, when a magnetic field is applied, we can calibrate all angles with respect to the field direction. In analogy with the more frequently employed reflection ellipsometry, the p- and s-polarisation directions are defined as being parallel and perpendicular to the magnetic field, respectively.

To calibrate the ellipsometer components, we use a standard residue calibration as described by de Nijs et al. [31] for reflection ellipsometry. In a similar way, it can be applied to our transmission configuration. The residue function R is defined by

$$R = 1 - \eta^2 + 4\eta^2\left(\frac{\tan(\Psi)\sin(\Delta)\tan(A)}{\tan^2(\Psi) + \tan^2(A)}\right)^2, \tag{3}$$

where A is the angle of the analyser, and η is a frequency dependent factor describing the difference in AC and DC attenuation of the electronics; generally it is found that $\eta < 1$. The angle A, which defines the reference plane, is found in the minimum of Eq. (3).

In Fig. 4 the measured residue is plotted as a function of the analyser angle A for different values of the applied magnetic field. As expected, the residue R does not depend on the analyser angle in the absence of an external magnetic field. In this case, the optical system comprising the cuvette with ferrofluid, is isotropic and the aforementioned p- and s-directions are not defined. Upon applying a very moderate magnetic field, an angle-dependence is observed. The residue exhibits a minimum, which is independent of the magnitude of the applied magnetic field. The minimum corresponds to the p-direction, the s-direction is perpendicular to it. The residue function R

[1] The absorbance is defined by $A = -^{10}\log(I/I_0)$. The extinction coefficient γ_{ext} is given by $I/I_0 = \exp(-\gamma_{ext} z)$ with I/I_0 the attenuation of the incident light with intensity I_0 at a depth z.

Table 1
Fit parameters corresponding to the solid lines in Fig. 4, obtained using the residue fit function in Eq. (3). Additionally, the values for birefringence and dichroism, obtained using Eqs. (8), are given

B (T)	η	$\tan(\Psi)$	Δ (°)	δn	δk
0.014	0.992	0.985	16.18	2.70×10^{-6}	1.44×10^{-7}
0.025	0.992	0.944	32.23	5.37×10^{-6}	5.50×10^{-7}
0.039	0.992	0.911	46.44	7.74×10^{-6}	8.90×10^{-7}

is symmetric with respect to the minimum, while the value of R increases with rising magnetic flux density. To obtain more quantitative information, we fitted the data in Fig. 4 using Eq. (3). The fitted curves are represented by the solid lines. The resulting fit parameters are summarised in Table 1.

The attenuation factor η does not depend on the applied magnetic field, as is to be expected for an experimentally defined quantity. The quantities $\tan(\Psi)$ and Δ determine the shape of the residue curve and exhibit a considerable variation with the applied magnetic flux density B. Details on the quantitative interpretation of $\tan(\Psi)$ and Δ in terms of linear magneto-optical properties will be discussed in the following section.

3.2. Linear birefringence and dichroism

To extract the linear birefringence and dichroism from our ellipsometry parameters $\tan(\Psi)$ and Δ in Eq. (2), we first consider the linearly polarised incident light, propagating along the z-direction, to be described by [32]

$$E_{\mathrm{p,s}}(z,t) = E^0_{\mathrm{p,s}} \exp\left(i\frac{2\pi}{\lambda}\tilde{n}z\right)\exp(-i\omega t), \tag{4}$$

in which p and s indicate the polarisation directions, $E^0_{\mathrm{p,s}}$ is the amplitude of the incident wave, $\tilde{n} = n + ik$ the complex refractive index, λ the wavelength in vacuum, and ω the angular frequency. As already described above, upon applying a magnetic field perpendicular to the direction of light propagation, the optical system, consisting of the cuvette filled with ferrofluid, becomes uniaxially anisotropic. The extraordinary direction is parallel, while the ordinary directions are perpendicular to the magnetic field. As a result of the calibration described in the previous section, the extraordinary and ordinary directions correspond directly to the p- and s-directions. The Jones matrix describing the transmission characteristics of such an anisotropic medium, also referred to as a linearly dichroic retarder [30], is given by

$$\begin{pmatrix} E'_{\mathrm{p}} \\ E'_{\mathrm{s}} \end{pmatrix} = \begin{pmatrix} \exp\left(i\frac{2\pi}{\lambda}\tilde{n}_{\mathrm{ex}}d\right) & 0 \\ 0 & \exp\left(i\frac{2\pi}{\lambda}\tilde{n}_{\mathrm{or}}d\right) \end{pmatrix} \begin{pmatrix} E_{\mathrm{p}} \\ E_{\mathrm{s}} \end{pmatrix}, \tag{5}$$

where $E_{\mathrm{p,s}}$ and $E'_{\mathrm{p,s}}$ represent the polarisation states of the incident and transmitted light, respectively. The complex refractive indices for the two anisotropy axes are represented by $\tilde{n}_{\mathrm{ex}}$ and $\tilde{n}_{\mathrm{or}}$, and d is the optical path length, i.e. the internal thickness of the cuvette. In fact, the diagonal terms of the Jones matrix in Eq. (5) are identical to the transmission coefficients $t_{\mathrm{p,s}}$ in Eq. (2) since

$$t_{\mathrm{p}} = \frac{E'_{\mathrm{p}}}{E_{\mathrm{p}}} = \exp\left(i\frac{2\pi}{\lambda}n_{\mathrm{ex}}d\right)\cdot\exp\left(-\frac{2\pi}{\lambda}k_{\mathrm{ex}}d\right), \tag{6a}$$

$$t_{\mathrm{s}} = \frac{E'_{\mathrm{s}}}{E_{\mathrm{s}}} = \exp\left(i\frac{2\pi}{\lambda}n_{\mathrm{or}}d\right)\cdot\exp\left(-\frac{2\pi}{\lambda}k_{\mathrm{or}}d\right). \tag{6b}$$

Structural anisotropy in a material generally gives rise to anisotropic optical properties. Linear birefringence and dichroism are related to differences in the real and imaginary parts of the complex refractive index for different directions, i.e. polarisation states, in a material. In our case of a ferrofluid in an external magnetic field, the linear birefringence and dichroism are given by

$$\delta n = n_{\mathrm{ex}} - n_{\mathrm{or}}, \tag{7a}$$

$$\delta k = k_{\mathrm{ex}} - k_{\mathrm{or}}, \tag{7b}$$

in which n_{ex} (n_{or}) and k_{ex} (k_{or}) are the real and imaginary parts of the complex refractive index in the extraordinary (ordinary) directions. Inserting Eqs. (6) into the complex reflection coefficient ρ (Eq. (2)), and using Eqs. (7), we obtain simple relations between the ellipsometry parameters $\tan(\Psi)$ and Δ:

$$\delta n = \frac{\Delta\cdot\lambda}{2\pi\cdot d}, \tag{8a}$$

$$\delta k = -\frac{\ln(\tan(\Psi))\cdot\lambda}{2\pi\cdot d}. \tag{8b}$$

Using these expressions, the linear magneto-optical properties can be readily derived from the experimentally determined ellipsometry parameters. For the Ψ and Δ values obtained from Fig. 4, the birefringence and dichroism values, calculated using Eqs. (8), are given in Table 1.

4. Experimental results

In one of the previous sections, we determined the values of Ψ and Δ from the residue calibration curves. It enables determination of the linear magneto-optical properties through Eqs. (8), but this procedure is quite elaborate and thus relatively slow. To determine birefringence and dichroism spectra, the analyser angle was set to 45°. This is the most logical choice since initially, before applying a field, the system is isotropic and t_{p} is equal to t_{s}, i.e. the components parallel and perpendicular to the magnetic field are equal.

In Fig. 5 the birefringence δn and dichroism δk are plotted as a function of wavelength for three values of the applied magnetic field. Below approximately 500 nm the optical absorption in the ferrofluid becomes so large that accurate measurements cannot be performed using the present combination of our Xe lamp and a relatively thick cuvette with an optical path length of 1 cm. As is well-known, for increasing magnetic flux densities the birefringence and dichroism both become larger. Furthermore, the birefringence shows a continuous decrease towards longer wavelengths, while the dichroism exhibits a minimum near 750 nm. This is very similar to the UV–vis absorbance curve in Fig. 3. In fact, from the absorbance data the imaginary part of the dielectric function k can be determined. We find that

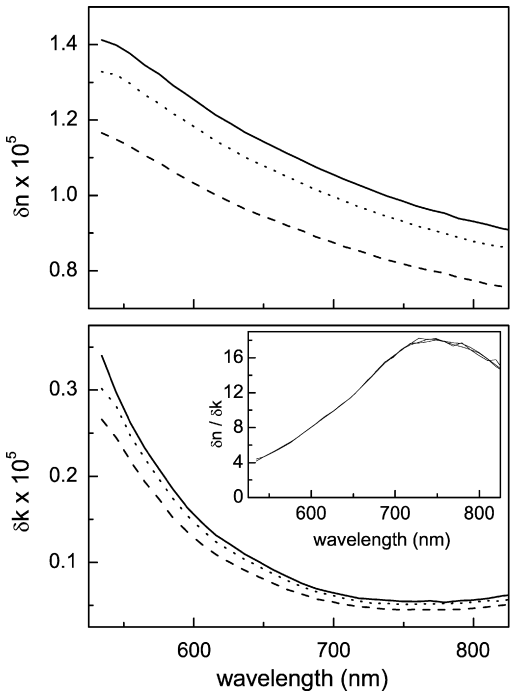

Fig. 5. Birefringence δn and dichroism δk as a function of wavelength for different strengths of the applied magnetic field. (- - -), (· · ·) and (—) correspond to magnetic flux densities of 0.17, 0.32 and 0.45 T, respectively. The inset shows the wavelength dependence of the ratio $\delta n/\delta k$. The fill fraction amounted to $\Phi = 2.18 \times 10^{-4}$.

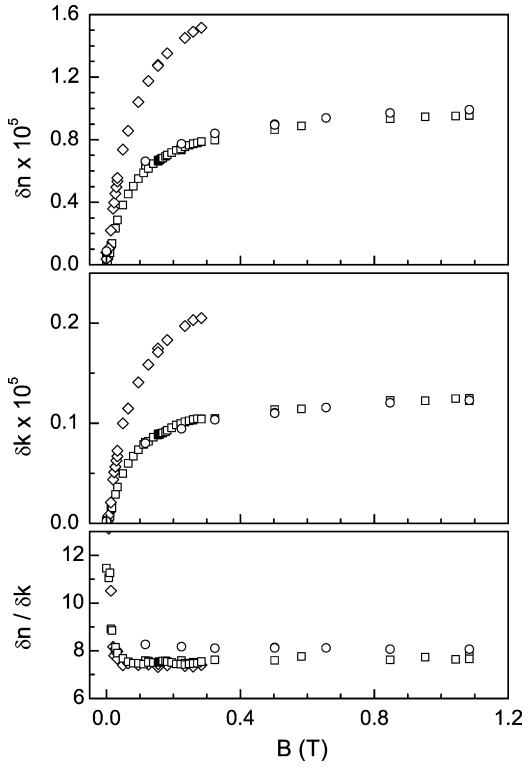

Fig. 6. Birefringence δn and dichroism δk as a function of magnetic flux density for different concentrations of ferrofluid. The fill fractions amounted to $\Phi = 1.56 \times 10^{-4}$ and 3.12×10^{-4} ((□) and (◇), respectively). For the larger concentration ($\Phi = 1.56 \times 10^{-3}$ (○)), the values of δn and δk were divided by 10. Also, to circumvent the significantly larger optical absorption at these high concentrations, a cuvette with an optical path length of 1 mm was used. The bottom panel shows the field-dependence of the ratio $\delta n/\delta k$. All measurements were performed at a wavelength of 600 nm.

for the magnetic field strengths considered in this work, the maximum value of the ratio $\delta k/k$ amounts to approximately 7%. Also the wavelength-dependent ratio of birefringence and dichroism $\delta n/\delta k$ is plotted. This ratio increases from a value of 4 on the short-wavelength side, to reach a maximum of 18 at approximately 750 nm, followed by a decline toward even longer wavelengths.

To further investigate the field dependence of the linear magneto-optical properties, in Fig. 6 the birefringence and dichroism are plotted as a function of the magnetic flux density for various concentrations at a wavelength of 600 nm.

For the highest concentration a thinner cuvet (1 mm optical path length) was used to ensure sufficient intensity on the detector side. As is evident from the data in Fig. 6, the birefringence and dichroism both scale linearly with concentration over the entire concentration range and also at all values of the field strength. For low fields both magneto-optical quantities δn and δk increase rapidly with the applied magnetic field. The frequently observed quadratic dependence on the applied field was not found in our results. Apparently, we did not go down to sufficiently low magnetic fields. For fields exceeding approximately 0.3 T, birefringence and dichroism approach their saturation value, which depend linearly on the concentration of magnetic nanoparticles in suspension.

In the bottom panel of Fig. 6, the ratio of δn and δk is shown to be independent of the magnetic field, except for very low flux densities (<0.1 T). The constant ratio $\delta n/\delta k \approx 8$ is in agreement with the value in the inset Fig. 5. For low flux densities, a strong increase is observed. This distinct rise may be attributed to particles of different sizes contributing to the magneto-optical properties. At low fields, only the larger particles (with a large magnetisation) are assumed to contribute to the magneto-optical effects, while for larger fields also the smaller particles (with smaller magnetisation) are responsible for the induced birefringence and dichroism. In case the contribution of small particles to δn and δk is different, a deviation can be envisaged.

In the ideal approximation of diluted suspensions, assuming there are no particle–particle interactions and in the absence of polydispersity, the variation of magneto-optical properties with the applied magnetic field strength is generally described by the second Langevin function [21,22]. For the birefringence, it is given by [19]

$$\delta n(H, d_0, s) = \delta n_s \frac{\int_0^\infty d^3 \left(1 - \frac{3L(\xi(d,H))}{\xi(d,H)}\right) f(d, d_0, s) dd}{\int_0^\infty d^3 f(d, d_0, s) dd}, \quad (9)$$

where $L(\xi(d, H)) = \coth(\xi) - 1/\xi$ represents the well-known Langevin function describing paramagnetic behaviour, with $\xi = \mu_0 m(d) H/k_B T$, μ_0 the permeability of vacuum, $m(d)$ the diameter-dependent magnetic moment of the particle, $H = B/\mu_0$ the strength of the applied magnetic field, k_B the Boltzmann constant and T the absolute temperature. The log-normal size-distribution f, given by Eq. (1), depends on the parame-

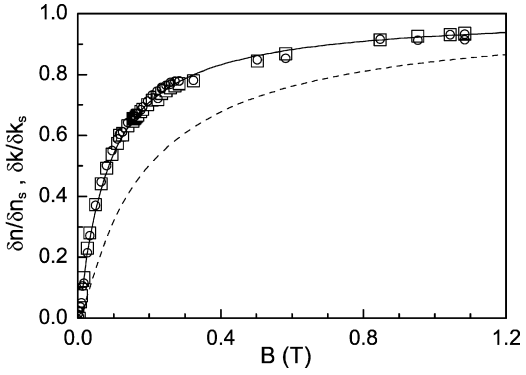

Fig. 7. Normalised birefringence $\delta n/\delta n_s$ (□) and dichroism $\delta k/\delta k_s$ (○) as a function of magnetic flux density. The lines correspond to calculations of the field dependence using a standard deviation $s = 0.31$ of the log-normal distribution (Eq. (1)) and average diameters $d_0 = 7.4$ and 5.6 nm ((—) and (- - -), respectively.)

ters d_0 and s. For a perfectly monodisperse suspension, the log-normal distribution is a delta-function, and Eq. (9) reduces to

$$\delta n = \delta n_s \left(1 - \frac{3L(\xi)}{\xi}\right). \tag{10}$$

A similar expression holds for the dichroism δk.

From Eq. (10), it follows that the saturation values for the birefringence δn_s and dichroism δk_s can be obtained by plotting δn and δk as a function $1/H$. In the high field limit, a linear relation is indeed obtained. For a fill fraction $\Phi = 1.56 \times 10^{-4}$ (squares, in Fig. 6), we find that $\delta n_s = 1.036 \times 10^{-5}$ and $\delta k_s = 1.34 \times 10^{-6}$.

In Fig. 7 the normalised birefringence and dichroism are plotted. Within experimental error both exhibit the same dependence on the magnetic flux density. The normalised linear magneto-optical parameters are also compared to calculations using Eq. (9), taking into account the log-normal size distribution, i.e. the polydispersity [21], as shown in Fig. 2. With the standard deviation $s = 0.31$ determined from the analysis of TEM images (such as Fig. 1), the normalised birefringence (or dichroism, both exhibit the same dependence on applied field B) is plotted for average diameters of $d_0 = 5.6$ and 7.4 nm. The calculation based on the latter value shows a remarkably good agreement with the experimental results. This indicates the importance of the anisotropy, i.e. the long axis of the magnetite particles, in the contribution to the magneto-optical behaviour of our ferrofluids.

5. Comparison with other work and established theories

5.1. Spectral dependence

In most work on magneto-optical properties of ferrofluids in general, which has been published during the past few decades, a strong emphasis is on the magnetic field-dependent optical properties. A few exceptions are the papers by Llewellyn [14] and Yusuf et al. [33]. In the former, the wavelength-dependent birefringence and dichroism of ferrofluids, consisting of (i) Fe_3O_4 in diester and (ii) Co in toluene, are presented

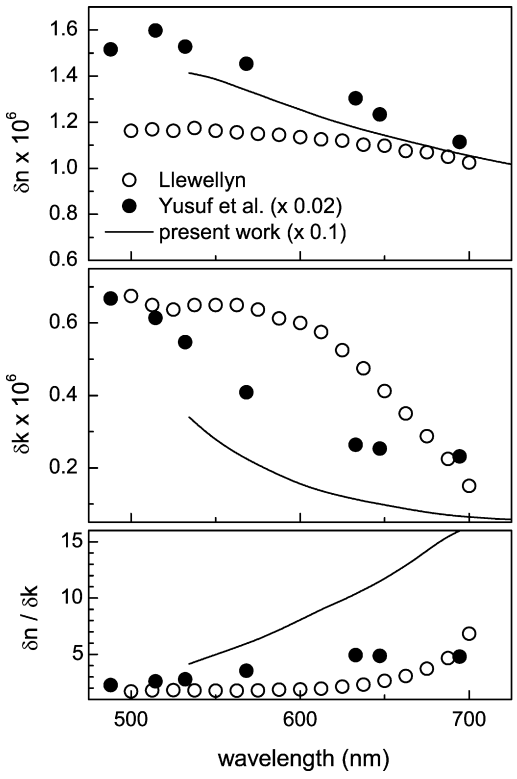

Fig. 8. Wavelength-dependent magneto-optical birefringence δn and dichroism δk of Fig. 5 (attenuated by a factor 10), compared to literature data presented by Llewellyn (open symbols) [14] and Yusuf et al. (closed symbols, attenuated by a factor 50) [33] for Fe_3O_4 ferrofluids. The fill fraction for the Yusuf-data amounts to $\Phi = 5.48 \times 10^{-4}$, while this value is not given in the Llewellyn-work. Only the data in the range of 500–700 nm are shown. The bottom panel shows the ratio $\delta n/\delta k$ as a function of wavelength.

in the range of 300–700 nm. The latter paper describes concentration and wavelength dependence of the magneto-optical properties of a magnetite ferrofluid.

The results from these publications are shown in Fig. 8 in the spectral range of 500–700 nm. Details on the suspension used by Llewellyn, such as particle size and fill fraction, are not provided. The experiments were performed at a relatively low magnetic flux of 0.075 T, which might explain the considerably lower values of δn and δk in their work as compared to our results in Fig. 5. The fill fraction for the results by Yusuf et al. amounts to $\Phi = 5.48 \times 10^{-4}$. In their case, the saturation values at 0.5 T were used for comparison.

Despite the difference of approximately one order of magnitude in the absolute values of birefringence and dichroism, most likely related to different concentrations and/or a lower applied field, there are a number of similarities between the various sets of data in the range of 500–700 nm. The decrease of the birefringence and the dichroism with increasing wavelength is observed in all experiments. In Fig. 5, considering the lowest applied field, the decrease of δn and δk amount to approximately 25 and 80%, respectively, while the two magneto-optical quantities in the Llewellyn-data in Fig. 8 decrease by approximately 15 and 80%. Similar changes of δn and δk (25%, resp. 65%) over this wavelength range are also found by Yusuf et al. Accordingly, the ratio $\delta n/\delta k$ of birefringence and dichro-

ism exhibits a 2.5–4-fold increase in both sets of literature data.

However, the spectral features, i.e. the 'shape' of the changes with wavelength are considerably different. One problem is that the bulk dielectric function of Fe_3O_4 is not well-documented in the literature, most likely owing to the difficulty of obtaining an accurate result. Full or partial oxidation of Fe_3O_4 to Fe_2O_3 with prolonged exposure to air will give rise to a mixing of contributions to the measured optical response. Additionally, it is well-known from other work on metallic nanoparticles [34] that the optical response of particles with dimensions in the low-nanometer range may be substantially different from their bulk counterparts. This may also be the case here. For the calculations presented in the next part of this section, we will use the bulk dielectric function as given by Schlegel et al. [35]. Finally, the surrounding medium also influences the spectral characteristics. Llewellyn used diester as solvent, while Yusuf et al. dispersed the particles in Isopar-M liquid. For the experiments presented in this work cyclohexane was used.

5.2. Field strength dependence

In contrast to the spectral characteristics of ferrofluid birefringence and dichroism a large amount of work has been done on the magnetic flux dependence [9–27]. For low fields, the well-known quadratic increase of magneto-optical properties has been reported frequently. Also, the high-field regime has been measured and analysed extensively. Our results presented in Figs. 6 and 7 are part of the last category, since we did not focus on the low-field limit.

The optical anisotropy of ferrofluids in the presence of an applied magnetic field has often been considered to be due to shape anisotropy of magnetic particles or particle-clusters. Differences between the various models often are due to the assumption of either magnetically induced of pre-existing agglomerates of particles. The first theoretical description of this shape anistropy was provided by Scholten [11], based primarily on the pioneering work of Skibin [9]. More recently, Raşa presented more general formula's for the magneto-optical properties [21,22]. For the fill fractions Φ (i.e. nanoparticle concentrations) considered in this work, the expressions by Raşa yield identical results as compared to the Scholten-work. The extraordinary and ordinary components ε_{ex} and ε_{or} of the ferrofluid dielectric function parallel and perpendicular to the applied magnetic field are derived by determining the dielectric tensor

$$\varepsilon_{ex} = \frac{(1-\Phi)\varepsilon_1 + \Phi(\varepsilon_\parallel + 2(\varepsilon_\perp - \varepsilon_\parallel)(L(\xi)/\xi))}{(1-\Phi) + (\Phi/\varepsilon_2)(\varepsilon_\parallel + 2(\varepsilon_\perp - \varepsilon_\parallel)(L(\xi)/\xi))}, \tag{11a}$$

$$\varepsilon_{or} = \frac{(1-\Phi)\varepsilon_1 + \Phi(\varepsilon_\perp + (\varepsilon_\parallel - \varepsilon_\perp)(L(\xi)/\xi))}{(1-\Phi) + (\Phi/\varepsilon_2)(\varepsilon_\perp + (\varepsilon_\parallel - \varepsilon_\perp)(L(\xi)/\xi))}, \tag{11b}$$

in which ε_1 is the real dielectric function of the solvent (cyclohexane in our case), ε_2 is the complex dielectric function of magnetite and

$$\varepsilon_\perp = \frac{\varepsilon_1\varepsilon_2}{\varepsilon_1 + (\varepsilon_2 - \varepsilon_1)n_\perp}, \tag{12a}$$

$$\varepsilon_\parallel = \frac{\varepsilon_1\varepsilon_2}{\varepsilon_1 + (\varepsilon_2 - \varepsilon_1)n_\parallel}. \tag{12b}$$

The depolarization factors $n_\parallel$ and $n_\perp$ for prolate ellipsoidal particles parallel and perpendicular to their long axis are given by

$$n_\parallel = \frac{1-e^2}{e^2}\left(\frac{1}{2e}\ln\left(\frac{1+e}{1-e}\right) - 1\right), \tag{13a}$$

$$n_\perp = \frac{1-n_\parallel}{2}, \tag{13b}$$

with the excentricity $e = \sqrt{1-\eta^2}$ defined by the ratio η of the short and long diameters. For the particles considered here, $\eta = 5.6\ \text{nm}/7.4\ \text{nm} = 0.76$, $e = 0.65$, yielding $n_\parallel = 0.26$ and $n_\perp = 0.37$.

A few years after the publication by Scholten [11], Taketomi presented a study of the magneto-optical effects in highly concentrated thin films of ferrite fluids [15]. The anomalous results observed in the experiments were attributed to rod-like chain formation and alignment of the ferrite particulate rods in the applied field. On the basis of these results, a dielectric tensor was derived, which also yields expressions for the parallel and perpendicular components of the dielectric functions

$$\varepsilon_{ex} = \varepsilon_1 + \alpha\Phi\frac{\varepsilon_2 - \varepsilon_1}{\varepsilon_2 + \varepsilon_1}\left(\varepsilon_2 + \varepsilon_1 - 2\varepsilon_2\frac{L(\xi)}{\xi}\right), \tag{14a}$$

$$\varepsilon_{or} = \varepsilon_1 + \alpha\Phi\frac{\varepsilon_2 - \varepsilon_1}{\varepsilon_2 + \varepsilon_1}\left(\varepsilon_2 + \varepsilon_1\frac{L(\xi)}{\xi}\right), \tag{14b}$$

where the dielectric functions ε_1 and ε_2 are identical to those used in the Raşa-expressions and $\alpha < 1$ is a constant of order unity representing the fraction of magnetic material, i.e. magnetite in our case, in the cylindrical rod-like aggregates. The expressions derived by Raşa [21] reduce to Eqs. (14) by setting the denominator in Eqs. (11) equal to 1, inserting the depolarization factors for an infinitely long cylinder ($n_\parallel = 0$ and $n_\perp = 0.5$) and replacing the magnetic moment of a particle by that of a rod-like aggregate. Despite the considerably lower concentrations in the ferrofluid used in this work, we also compare our experimental results to calculations using this model.

Using the anisotropic dielectric functions as derived by Raşa and Taketomi, the calculation of the linear magneto-optical properties is straightforward. Since $n_{ex} = \text{Re}(\sqrt{\varepsilon_{ex}})$, $n_{or} = \text{Re}(\sqrt{\varepsilon_{or}})$, $k_{ex} = \text{Im}(\sqrt{\varepsilon_{ex}})$, and $k_{or} = \text{Im}(\sqrt{\varepsilon_{or}})$, Eqs. (8) immediately yield the linear birefringence and linear dichroism.

Before turning our attention to the field strength-dependent magneto-optical properties, the equations by Raşa and Taketomi (Eqs. (11) and (14)) enable determination of the ratio $\delta n/\delta k$ as a function of wavelength, using the dielectric function of bulk magnetite. The ratio does not exhibit any dependency on the applied magnetic field. In Fig. 9 the bulk Fe_3O_4 dielectric function is shown in the top panel. In the same figure, the ratio of birefringence and dichroism are shown as calculated from Eqs. (11) derived by Raşa and Eqs. (14) by Taketomi using the bulk dielectric function. Despite the similarity of the two calculated wavelength-dependent ratios, comparison of them to the experimental results in Figs. 5 and 8 reveals enormous differences. Where all experiments exhibit a continuous increase of the ratio $\delta n/\delta k$ with wavelength, the calculated spectra show a

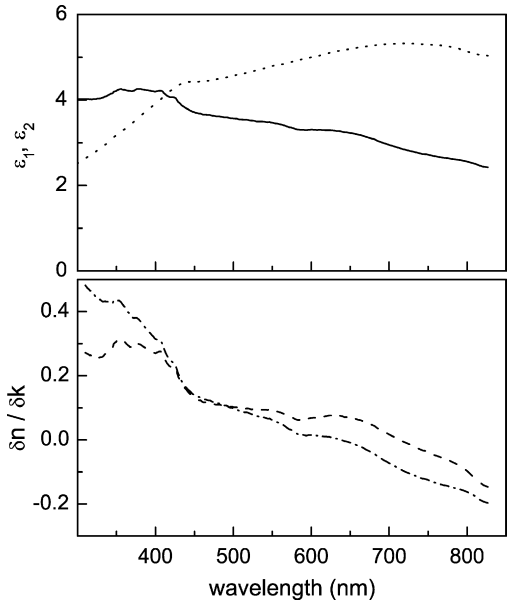

Fig. 9. (Top) Wavelength-dependent real (—) and imaginary (···) parts of the dielectric function of bulk Fe_3O_4 as taken from the work by Schlegel et al. [35]. (bottom) Ratio $\delta n/\delta k$ of birefringence δn and dichroism δk as a function wavelength, calculated using the expressions given by Raşa and Taketomi ((- - -) and (-···-), respectively) [15,21].

cross-over from positive to negative values. But most obvious is the order of magnitude difference between measured and calculated spectral dependencies, which is most pronounced for our experimental results presented in this work. This marked deviation between experiment and theory is most likely due to the fact that the bulk dielectric function of magnetite can not be used for the Fe_3O_4 nanoparticles in the ferrofluids considered in all experiments, as already described in the previous section. Furthermore, the bulk dielectric function shown in the top panel of Fig. 9 is also not even in qualitative agreement with the absorbance spectra depicted in Fig. 3.

The size-dependence of the optical properties of nanoparticles as compared to that of bulk material, may also explain the strong increase of the ratio of birefringence and dichroism observed in our present work (Fig. 6) for lower fields. At low applied fields only the large particles are influenced by the external applied field, while the smaller particles still are randomly oriented in the ferrofluid. Upon increasing the field, the smaller particles, with different dielectric and/or magneto-optical properties, also start to contribute to the birefringence and dichroism.

Using Eqs. (11) and (14), we also calculated the magnetic field-dependent magneto-optical properties as shown in Fig. 6. In these calculations we inserted the known fill fractions Φ of our ferrofluid samples, and the dielectric functions $\varepsilon_1 = 2.03$ and $\varepsilon_2 = 3.30 + 5.00i$ of cyclohexane and bulk magnetite, respectively, at a wavelength of 600 nm. A very similar qualitative field-dependence is observed in calculations as compared to the experiments. But as with the spectral dependence of the magneto-optical properties, also the theoretical field-dependent birefringence and dichroism do not show quantitative agreement with the experiments.

As mentioned above, we ascribe these considerable discrepancies to the modified bulk dielectric function of magnetite for the nanoscale particles in ferrofluids. To obtain an indication of this modification, required to achieve quantitative agreement, we used the Raşa and Taketomi models to fit the dielectric function for our nanoparticulate suspensions. To simplify the calculations, we do not take into account polydispersity here.

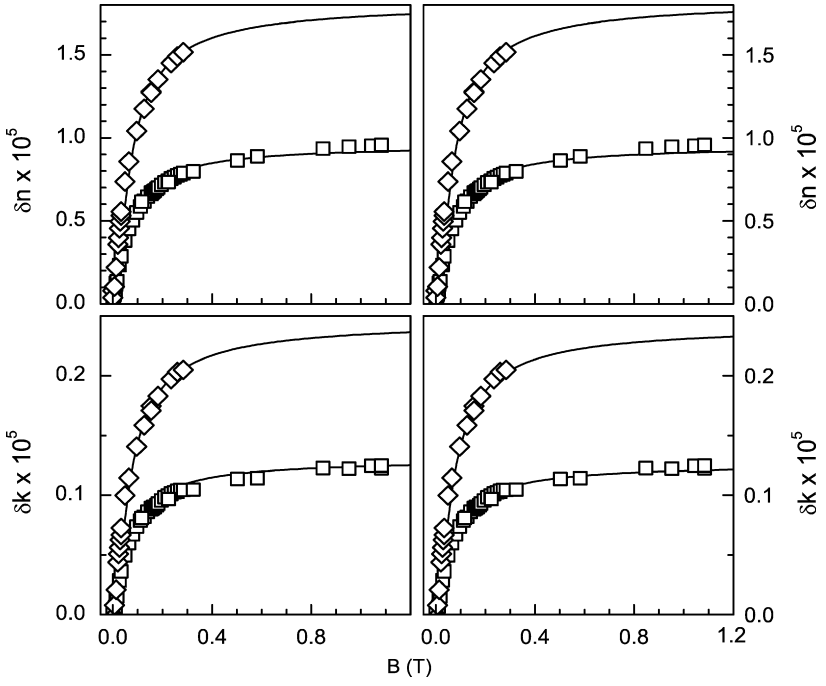

Fig. 10. Comparison of experimentally determined birefringencence δn (top) and dichroism δk (bottom) for fill fractions of $\Phi = 1.56 \times 10^{-4}$ and 3.12×10^{-4} ((□) and (◇), respectively) to calculations using the Raşa equations (11) (left) and Taketomi equations (14) (right), as described in the text.

The results are shown in Fig. 10. Using the expressions of Raşa and the fill fractions $\Phi = 1.56 \times 10^{-4}$ and 3.12×10^{-4}, as indicated in Fig. 6, very good quantitative agreement is obtained, as shown in the left panels of Fig. 10, for an effective magnetite dielectric function $\varepsilon_2 = 4.5 + 0.23i$. The real part of this dielectric constant (at a wavelength of 600 nm) is still of the same order of magnitude but 40% higher than the bulk value, but the imaginary part is considerably reduced by an order of magnitude. Similarly, the expressions of Taketomi also yield a good correspondence as shown in the right panels of Fig. 10. In the latter case a dielectric function $\varepsilon_2 = 4.2 + 0.245i$ is obtained by fitting, very similar to that obtained from the Raşa model. However, as described above, the equations by Taketomi also contain a factor α representing the fraction of magnetite in the rod-like aggregates. A proper fit is found for $\alpha = 0.12$. This value indicates rather low magnetite quantities in the rod-like aggregates due to chain formation. Furthermore, it may also reflect that not all magnetite particles are aggregated. Large separations and thus small interactions between neighbouring magnetite particles in the chain-like aggregates suggest that chaining is not an issue in our experiments. This is in agreement with the low concentrations, i.e. fill fractions of our ferrofluid, as compared to those used by Taketomi [15].

Finally, the magnetic field-dependent experiments presented here for a wavelength of 600 nm, can in principle be performed at all wavelengths. As such, it enables determination of the effective dielectric function at all photon energies and thus allows spectral characterisation of magnetic nanoparticle suspensions. However, a precise determination of the dielectric function of Fe_3O_4 lies outside the scope of the present work.

6. Conclusions

We have explored the versatility of spectroscopic ellipsometry in transmission mode to study magneto-optical properties of magnetite ferrofluids. Linear birefringence and linear dichroism are both obtained simultaneously from measured ellipsometric quantities Ψ and Δ as a function of applied magnetic fields up to 1.1 T. We derive simple equations, which relate the magneto-optical properties to the experimentally obtained optical quantities. Since we are able to measure birefringence and dichroism at the same time with high accuracy, and as a function of the wavelength of the light, we can compare our data to previous experimental work and also to theoretical models describing the magneto-optical characteristics of ferrofluids.

The spectral characteristics of the birefringence and dichroism are in line with previous experimental work. However, marked differences are observed which may be related to size distribution of the particles, the solvent in which they are suspended, the degree of oxidation of the magnetite particles and the effective dielectric function of the nanoparticles constituting the ferrofluids. Most pronounced is the large ratio of birefringence and dichroism in our results as compared to previous work. The magnetic field-dependent optical response is in qualitative agreement both with previous experimental work and also with theoretical models. The quantitative discrepancies between our experimental results and the theoretical models have been discussed in relation to a modified dielectric function of the magnetite nanoparticles in the ferrofluids.

Acknowledgments

We thank M. Raşa, M.P.B. van Bruggen and H. Wormeester for helpful discussions. This work is part of the research program of the Stichting voor Fundamenteel Onderzoek der Materie (FOM), financially supported by the Nederlandse Organisatie voor Wetenschappelijk Onderzoek (NWO).

References

[1] Q. Majorana, C. R. Hebd. Acad. Sci. 135 (1902) 159–161.
[2] Q. Majorana, C. R. Hebd. Acad. Sci. 135 (1902) 235–237.
[3] A. Cotton, H. Mouton, C. R. Hebd. Acad. Sci. 141 (1905) 317–319.
[4] P. Berger, N. Adelman, K. Beckman, D. Campbell, A. Ellis, G. Lisensky, J. Chem. Educ. 76 (1999) 943–948.
[5] D. Bica, L. Vekas, M. Raşa, J. Magn. Magn. Mater. 252 (2002) 10–12.
[6] G.A. van Ewijk, G.J. Vroege, A.P. Philipse, J. Magn. Magn. Mater. 201 (1999) 31–33.
[7] R. Massart, E. Dubois, V. Cabuil, E. Hasmonay, J. Magn. Magn. Mater. 149 (1995) 1–5.
[8] M. Shinkai, J. Biosci. Bioeng. 94 (2002) 606–613.
[9] Y.N. Skibin, V.V. Chekanov, Y.L. Raikher, Zh. Eksp. Teor. Fiz. 72 (1977) 949–955.
[10] H.W. Davies, J.P. Llewellyn, J. Phys. D Appl. Phys. 12 (1979) 311–319.
[11] P.C. Scholten, IEEE Trans. Magn. 16 (1980) 221–225.
[12] H.W. Davies, J.P. Llewellyn, J. Phys. D Appl. Phys. 13 (1980) 2327–2336.
[13] P.C. Scholten, J. Phys. D Appl. Phys. 13 (1980) L231–L234.
[14] J.P. Llewellyn, J. Phys. D Appl. Phys. 16 (1983) 95–104.
[15] S. Taketomi, Jpn. J. Appl. Phys. 22 (1983) 1137–1143.
[16] J.J.M. Janssen, J.A.A.J. Perenboom, J. Magn. Magn. Mater. 81 (1989) 14–24.
[17] P. Daveze, H. Sahsah, J. Monin, Meas. Sci. Technol. 7 (1996) 157–161.
[18] M. Xu, P.J. Ridler, J. Appl. Phys. 82 (1997) 326–332.
[19] E. Hasmonay, E. Dubois, J.-C. Bacri, R. Perzynski, Y. Raikher, V. Stepanov, Eur. Phys. J. B 5 (1998) 859–867.
[20] H.E. Horng, C.-Y. Hong, H.C. Yang, I.J. Jang, S.Y. Yang, J.M. Wu, S.L. Lee, F.C. Kuo, J. Magn. Magn. Mater. 201 (1999) 215–217.
[21] M. Raşa, J. Magn. Magn. Mater. 201 (1999) 170–173.
[22] M. Raşa, Eur. Phys. J. E 2 (2000) 265–275.
[23] E. Hasmonay, J. Depeyrot, M.H. Sousa, F.A. Tourinho, J.-C. Bacri, R. Perzynski, Y.L. Raikher, I. Rosenman, J. Appl. Phys. 88 (2000) 6628–6635.
[24] V. Buzmakov, A.F. Pshenichnikov, Colloid J. 63 (2001) 305–312.
[25] C.P. Pang, C.T. Hsieh, J.T. Lue, J. Phys. D Appl. Phys. 36 (2003) 1764–1768.
[26] A.F. Bakuzis, K.S. Neto, P.P. Gravina, L.C. Figueiredo, P.C. Morais, L.P. Silva, R.B. Azevedo, O. Silva, Appl. Phys. Lett. 84 (2004) 2355–2357.
[27] V. Socoliuc, D. Bica, J. Magn. Magn. Mater. 289 (2005) 177–180.
[28] R.J. Hunter, Foundations of Colloid Science, Oxford Univ. Press, New York, 2001.
[29] J.M.M. de Nijs, Ph.D. thesis, University of Twente, Enschede, The Netherlands (1989).
[30] R.M.A. Azzam, N.H. Bashara, Ellipsometry and Polarized Light, North Holland, Amsterdam, 1987.
[31] J.M.M. de Nijs, A.H.M. Holtslag, A. Hoekstra, A. van Silfhout, J. Opt. Soc. Am. A 5 (1988) 1466–1471.

[32] H.G. Tompkins, W.A. McGahan, Spectroscopic Ellipsometry and Reflectometry, A User's Guide, Wiley, New York, 1999.
[33] N.A. Yusuf, A. Ramadan, H. Abu-Safia, J. Magn. Magn. Mater. 184 (1998) 375–386.
[34] U. Kreibig, M. Vollmer, Optical Properties of Metal Clusters, Springer-Verlag, Berlin, 1995.
[35] A. Schlegel, S.F. Alvarado, P. Wachter, J. Phys. C Solid State Phys. 12 (1979) 1157–1164.